

Heavy Dark Matter Through the Higgs Portal

John March-Russell¹, Stephen M. West^{1,2}, Daniel Cumberbatch³ and
Dan Hooper⁴.

¹*Theoretical Physics, Department of Physics
University of Oxford, 1 Keble Road, Oxford OX1 3NP, UK*

²*Magdalen College, Oxford, OX1 4AU, UK*

³*Astrophysics Dept., University of Oxford,
Denys Wilkinson Building, Oxford OX1 3RH, UK*

⁴*Center for Particle Astrophysics, Fermi National Accelerator Laboratory, Batavia, IL
60510-0500, USA*

(January 22, 2008)

Abstract

Motivated by Higgs Portal and Hidden Valley models, heavy particle dark matter that communicates with the supersymmetric Standard Model via pure Higgs sector interactions is considered. We show that a thermal relic abundance consistent with the measured density of dark matter is possible for masses up to ~ 30 TeV. For dark matter masses above ~ 1 TeV, non-perturbative Sommerfeld corrections to the annihilation rate are large, and have the potential to greatly affect indirect detection signals. For large dark matter masses, the Higgs-dark-matter-sector couplings are large and we show how such models may be given a UV completion within the context of so-called “Fat-Higgs” models. Higgs Portal dark matter provides an example of an attractive alternative to conventional MSSM neutralino dark matter that may evade discovery at the LHC, while still being within the reach of current and upcoming indirect detection experiments.

1 Introduction

Recently, there has been a surge of interest in models where the Standard Model (SM) or the Minimal Supersymmetric Standard Model (MSSM) communicates with a partially hidden sector via either Z' or Higgs interactions [1, 2, 3, 4, 5, 6]. These Hidden Valley or Higgs Portal models provide a stimulating and consistent alternative to the usual model building assumption of a desert above the weak scale. Higgs-sector and Z' interactions between the hidden sector and the SM states are special in that they involve gauge-invariant operators of dimension $d_O \leq 4$, and thus can be induced by physics at arbitrarily high scales with unsuppressed couplings. In the case of a Z' the interactions can either occur directly with SM states if they are charged under the $U(1)'$ or, possibly more interestingly, indirectly due to a kinetic-mixing term, $\epsilon F_Y^{\mu\nu} F'_{\mu\nu}$, between hypercharge and the new $U(1)$, in which case ϵ , and thus the effective size of the SM-hidden sector interaction, can be suppressed [7, 1, 6]. On the other hand, in the case of the Higgs-sector interactions of interest to us here, couplings of the form $|H|^2 s^2$ involving the SM or MSSM Higgs states and new SM gauge singlet states can be large, especially in the situation where the TeV-scale theory UV-completes not far above the weak scale to a strongly interacting theory with light composite states.

It is interesting to ask whether such models lead to new dark matter candidates with qualitatively different phenomenology. In this paper we argue that dark matter communicating with a supersymmetrized SM purely via Higgs-sector interactions (the Higgs Portal) leads to new and unusual features.¹ First, as we will show, the thermal relic abundance in such a scenario can be consistent with the measured density of dark matter for masses as high as ~ 30 TeV, much larger than are usually considered (while also being consistent with the upper bound on the mass of thermal relic dark matter derived from unitarity [11]). Second, for dark matter masses above ~ 1 TeV non-perturbative Sommerfeld corrections [12] to the low-velocity annihilation rate are large. Several authors have recently recognised the potential importance of these corrections to the dark matter relic density calculations [13, 14, 15, 16], which lead to enhanced annihilation rates in the case of attractive interactions. Even more importantly, as we will argue in detail in a companion paper [17], these corrections have the potential to greatly enhance the indirect annihilation signals by factors of up to 10^5 beyond those predicted without consideration of the Sommerfeld factor, potentially leading to a significant change in the optimal search strategy.

As well as providing examples in which the dark matter particle is beyond the kinematic reach of the Large Hadron Collider (LHC) but is potentially detectable by indirect and direct dark matter searches, the models presented here are independently motivated by the desire to raise the MSSM upper bound on the lightest Higgs mass, and so relax the current tension with the LEP2 Higgs-mass exclusion limit. It is also interesting that our models may be given a UV completion in so-called “Fat-Higgs” models [18]² in which some TeV-scale states are composites of the underlying strong-coupling dynamics. This

¹Other works which consider aspects of dark matter phenomenology in the context of Hidden Valley or Higgs Portal models are contained in Ref. [8, 9], while earlier related studies are contained in Ref. [10].

²Other models in a similar class to the Fat Higgs model are discussed in Ref. [19].

UV completion is consistent with both collider constraints and aesthetic requirements such as gauge coupling unification. This completion is discussed in detail in Section 6.

Furthermore, the existence of partially hidden (secluded) sectors is common in models that attempt to embed the SM within a larger structure. Well studied examples include higher-rank GUT models, such as those based upon E_6 [20], and supersymmetry breaking models, in particular the messenger sectors of gauge-mediated supersymmetry breaking models [8]. More recently, it has been argued that secluded or hidden sectors in the form of Randall-Sundrum-like warped “throats” [21] are a ubiquitous feature of the landscape of string compactifications [22], thus implying that there is not an insignificant probability that a hidden or secluded throat with a mass scale close to the weak scale exists. In fact, as argued by Patt and Wilczek [4], the scales in sectors interacting by Higgs portal interactions are commonly tied together.

Naturally, if our dark matter candidate is to be the dominant component of the cosmological dark matter, we must ensure that the usual neutralino dark matter candidate of the MSSM leads either to a subdominant relic density or is unstable. In the case in which R -parity is conserved and a neutralino is the lightest supersymmetric particle (LSP), the thermally generated abundance of such a state is in many models well below the measured dark matter density. In particular, wino-like or higgsino-like LSPs annihilate very efficiently, leading to subdominant abundances [23]. Coannihilations with other supersymmetric states can also deplete the neutralino abundance in many models [24]. Alternatively, instead of being a neutralino, the LSP could be a different supersymmetric state, such as a gravitino. Within the context of gauge-mediated supersymmetry breaking, for example, the LSP is typically a light gravitino which constitutes only a very small fraction of the cosmological dark matter abundance. On the other hand, if there exist R -parity violating interactions, then the LSP will be unstable thus evading this issue entirely.³

Turning to the structure of our paper, in Section 2 we introduce our models and explain how they are a modified form of the so-called Minimal Non-minimal Supersymmetric Standard Model (MNSSM), while in Section 3 we give a brief introduction to the physics of the Sommerfeld enhancement that plays an important role in our calculations. In Section 4 we summarize the calculation of the relevant dark matter annihilation cross section including the Sommerfeld enhancement and present our results for the relic density. In Section 5 we briefly discuss the direct and indirect detection of our dark matter candidate, leaving a more detailed study for a companion paper [17]. Section 6, in which we demonstrate that our models may be given a UV completion in so-called “Fat-Higgs” models where the states are composites of underlying strongly coupled dynamics, is somewhat outside the main development of our paper and may be skipped by readers only interested in dark matter phenomenology. Finally, our conclusions are given in Section 7.

³A late-decaying LSP may even be beneficial in that it can correct the BBN prediction for the ${}^6\text{Li}$ to ${}^7\text{Li}$ ratio [25].

2 The Supersymmetric Higgs Portal Model

The relevant terms of the model that we wish to study are specified by the superpotential

$$W = W_{MSSM}(\mu = 0) + \lambda N H_u H_d + \frac{\lambda'}{2} N S^2 + \frac{m_{\tilde{s}}}{2} S^2 + \dots, \quad (1)$$

where N and S are SM singlets and N gets an electroweak-sized scalar vacuum expectation value (vev). The term $W_{MSSM}(\mu = 0)$ refers to the MSSM superpotential without the “ μ ” term, while the ellipsis denote terms, such as possible tadpoles, that will not be important. S has an exact non-R Z_2 symmetry which will be unbroken in the vacuum and which leads to a stable relic, \tilde{s} , the fermionic component of the S superfield with mass $m_{\tilde{s}}$. Note that N does not have a mass term before electroweak symmetry is broken. In fact the masslessness of N before EWSB is not crucial; all that is required is that the mass of N is small compared to S as we explain in detail below. We will assume that the standard neutralino supersymmetric dark matter candidate is irrelevant, either because R_p is broken, or because its relic density is subdominant to that of \tilde{s} . This model Eq.(1) is a simple variation of the model outlined in Refs. [27] and [28], referred to as the Minimal Non-minimal Supersymmetric Standard Model (MNSSM) in Ref. [27], where the superpotential has the form $W_{MNSSM} = W_{MSSM}(\mu = 0) + \lambda N H_u H_d + t_2 N$, and t_2 is a mass dimension two “tadpole”-term parameter that is in general possible.

The annihilation cross sections determining the number density of our dark matter particle will depend on the couplings, λ and λ' . As we will argue in later sections, the most interesting dark matter phenomenology occurs when the coupling λ' is large. Furthermore, for large λ there are important additional contributions to the higgs quartic-self-couplings and the upper bound on the lightest higgs mass is considerably raised.

For sufficiently large λ, λ' couplings the theory Eq.(1) hits a Landau pole below the Planck-scale, and so must be considered a low-energy effective theory with a cutoff Λ . We will argue in Section 6 that the above effective theory can result from a limit of the Fat Higgs model [18] in which S is a composite meson field of new supersymmetry-preserving strong-interaction dynamics, giving our effective theory a possible and plausible UV completion without tadpole problems, and also with a natural reason to expect large couplings λ and λ' . We emphasize that the Fat Higgs model is only one of many possible examples of a UV completion with large couplings λ and λ' . To analyse the dark matter phenomenology it is sufficient to focus on the effective superpotential in Eq.(1) rather than that of any particular UV completion. Although the precise form of the superpotential, Eq.(1), arises as a low-energy limit of the Fat Higgs model, other terms, such as a bare μ -term, a mass term for N , or N^3 self-interactions can be added to Eq.(1) without qualitatively changing our results if the final mass of N is parametrically smaller than $m_{\tilde{s}}$ by a factor of $\mathcal{O}(10)$.⁴ We assume this in the remainder of our analysis.

From the superpotential, Eq.(1), the Lagrangian terms determining the important

⁴More precisely, the spectrum of neutral Z_2 -even Higgs scalars arising from H_u, H_d, N after mixing must be such that a state with substantial interaction with the Z_2 -odd states s, \tilde{s} has mass which is parametrically small compared to $m_{\tilde{s}}$.

interactions and masses in the model are

$$\mathcal{L} = \mathcal{L}_{\text{fermion}} + \mathcal{L}_{\text{scalar}}, \quad (2)$$

where,

$$\begin{aligned} \mathcal{L}_{\text{ferm}} &= -\lambda n \tilde{h}_u \tilde{h}_d - \lambda \tilde{n} \tilde{h}_u h_d - \lambda \tilde{n} h_u \tilde{h}_d - \frac{\lambda'}{2} n \tilde{s} \tilde{s} - \lambda' \tilde{n} \tilde{s} s - \frac{m_{\tilde{s}}}{2} \tilde{s} \tilde{s} + \text{h.c.} + \dots \\ \mathcal{L}_{\text{scal}} &= |\lambda' n s + m_{\tilde{s}} \tilde{s}|^2 + \left| \lambda h_u h_d + \frac{\lambda'}{2} s^2 \right|^2 + |\lambda n h_d + \lambda_t \tilde{t}_L \tilde{t}_R|^2 + |\lambda n h_u|^2 \\ &\quad + \text{soft susy breaking terms} + \dots \end{aligned}$$

where n (\tilde{n}), s (\tilde{s}), h_u (\tilde{h}_u) and h_d (\tilde{h}_d) are the scalar (fermionic) components of the superfields N , S , H_u and H_d respectively.

To simplify the analysis, we make the reasonable assumption that the scalar tri-linear A-terms and bilinear B-terms are small and consequently we neglect their effects in cross sections. In particular we are setting the tri-linear A-terms, $A_\lambda = A_{\lambda'} = 0$. We also neglect the D-term interactions as these give irrelevant 4-point Higgs interactions.

To assess the viability of our dark matter candidate, we need to calculate its thermal relic abundance. An important point to note is that the freeze-out temperature of our dark matter particle is higher than the electroweak phase transition temperature, T_c , for the range of dark matter masses $m_{\tilde{s}} \gtrsim 3 \text{ TeV}$ we consider. (In our companion paper [17] we will explore the region of dark matter masses below 3 TeV.) Consequently, in the relic density calculation, electroweak symmetry is still a good and no Higgs scalars will have vevs. Moreover, above T_c , the fermionic states \tilde{n} , \tilde{h}_u and \tilde{h}_d are massless, as are all quarks and gauge bosons. The only massive fermionic state of interest is \tilde{s} with mass $m_{\tilde{s}}$. In the scalar sector, the thermally-corrected masses of the scalar n states and MSSM Higgs bosons are taken to be negligible compared to $m_{\tilde{s}}$, which is a good approximation for the parameter range we are interested in.

Taking $m_{\tilde{s}} \gtrsim 3 \text{ TeV}$ does lead to one slight complication in our analysis in that the scalar state, s , has a very similar Boltzman factor compared to \tilde{s} near the freeze-out temperature, T_f . This is due to the fact that the mass splitting between s and \tilde{s} is small

$$m_s - m_{\tilde{s}} = (m_{\tilde{s}}^2 + m_{\text{susy}}^2)^{1/2} - m_{\tilde{s}} \simeq m_{\text{susy}}^2 / m_{\tilde{s}} < T_f \simeq m_{\tilde{s}} / 25, \quad (3)$$

where m_{susy} is the supersymmetry breaking scale, which is parametrically smaller than $m_{\tilde{s}}$. This means that the scalar s and fermion \tilde{s} states will freeze-out at roughly the same temperature and we have to consider the annihilation rates of the scalar states as well as the fermionic states⁵.

In addition to the purely scalar interactions which follow from Eq.(3) the fermionic interactions which are of importance in determining the relic abundance of our dark

⁵We remark in passing that our qualitative conclusions regarding the dark matter freeze out density would not be changed if a scalar component of S were the lightest Z_2 -odd state, say due to CP-violation. The Sommerfeld effect acts equally for both scalar and fermionic annihilating particles as explained in Section 3.

matter state are

$$\begin{aligned}
& \frac{1}{\sqrt{2}}(\lambda\phi_n(\tilde{h}_{uM}^0)^T C\tilde{h}_{dM}^0 + i\lambda a_n(\tilde{h}_{uM}^0)^T C\gamma_5\tilde{h}_{dM}^0 + \lambda\phi_u(\tilde{h}_{dM}^0)^T C\tilde{n}_M + i\lambda a_u(\tilde{h}_{dM}^0)^T C\gamma_5\tilde{n}_M) \\
& + \frac{1}{\sqrt{2}}(\lambda\phi_d(\tilde{h}_{uM}^0)^T C\tilde{n}_M + i\lambda a_d(\tilde{h}_{uM}^0)^T C\gamma_5\tilde{n}_M - \lambda'\phi_s\tilde{s}_M^T C\tilde{n}_M - i\lambda'a_s\tilde{s}_M^T C\gamma_5\tilde{n}_M) \\
& - \frac{1}{2\sqrt{2}}(\lambda'\phi_n\tilde{s}_M^T C\tilde{s}_M + i\lambda'a_n\tilde{s}_M^T C\gamma_5\tilde{s}_M) \\
& - \frac{1}{\sqrt{2}}(\phi_n[\overline{\tilde{h}_{uD}^-} P_L\tilde{h}_{dD}^- + \overline{\tilde{h}_{dD}^-} P_R\tilde{h}_{uD}^-] + ia_n[\overline{\tilde{h}_{uD}^-} P_L\tilde{h}_{dD}^- - \overline{\tilde{h}_{dD}^-} P_R\tilde{h}_{uD}^-]) \\
& - h_d^-\overline{\tilde{h}_{uD}^-} P_L\tilde{n}_M - (h_d^-)^*\tilde{n}_M^T C P_R\tilde{h}_{uD}^- - (h_u^+)^*\overline{\tilde{h}_{dD}^-} P_L\tilde{n}_M - h_d^+\tilde{n}_M^T C P_R\tilde{h}_{dD}^-,
\end{aligned}$$

where $P_{L,R} = (1 \pm \gamma_5)/2$ and we have rewritten the fermionic states in terms of Majorana and Dirac spinors indicated by the subscripts M and D respectively. The scalar states have been written in terms of their CP-odd and CP-even components, denoted generically as $A_i = \frac{1}{\sqrt{2}}(\phi_i + ia_i)$, and C is the charge conjugation matrix. The subscripts u and d on the scalars refer to the Higgs ‘‘up’’ and ‘‘down’’ states.

3 The Sommerfeld Enhancement

For dark matter particles moving at small relative velocities, the exchange of scalar states leads to an enhancement by factors depending on the inverse velocity, $1/v$. This Sommerfeld enhancement corresponds to the summation of a series of ladder diagrams where the scalar state is repeatedly exchanged (see Fig. 1). This enhancement is only significant if there exists an S -wave annihilation amplitude, otherwise the angular momentum barrier will suppress the effect.⁶

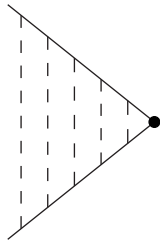


Figure 1: Generic Sommerfeld diagram. The ‘‘blob’’ vertex represents all possible S -wave annihilations of the incoming states including s-channel, t-channel and annihilation via contact interactions.

The calculation of the Sommerfeld enhancement can be formulated in terms of a non-relativistic quantum two-body problem with a potential acting between the incoming particles. This is equivalent to the distorted Born-wave approximation common in nuclear

⁶If vector states are exchanged, there can either be an enhancement or suppression depending on the relative charges of the annihilating particles.

physics. To a good approximation this leads to a dressing of the S -wave part of the tree-level cross sections with a multiplicative factor,

$$\sigma = R\sigma_{tree}^{\ell=0}. \quad (4)$$

The full calculation of R can be involved and in many cases, including that of a Yukawa potential, cannot be solved analytically. In our model the only particles which can act as the “rungs on the ladder” in the Sommerfeld diagram shown in Fig. 1 are the scalar n states, the \tilde{n} fermions not contributing to the enhancement. The non-relativistic potential which is relevant for all the diagrams we will consider is found to be

$$V = -\frac{\lambda'^2}{8\pi r}e^{-m_n r}, \quad (5)$$

where m_n is the mass of the particle acting as the “rungs on the ladder”. The Schrödinger equation for the two dark matter particle state, ψ , with this potential reads

$$-\frac{1}{m_{\tilde{s}}} \frac{d^2\psi}{dr^2} + V.\psi = K\psi, \quad (6)$$

where $K = Mv^2$ is the kinetic energy of the two dark matter particles in the center-of-mass frame, where each dark matter particle has velocity v . Using the outgoing boundary conditions, $\psi'(\infty)/\psi(\infty) = im_s v$, R is given as $R = |\psi(0)/\psi(\infty)|^2$. In the simple case we are considering, we can derive an analytic form for R . In the limit where the ratio $\epsilon \equiv m_n/m_{\tilde{s}} = 0$, R takes the form [16],

$$R = \frac{y}{1 - e^{-y}}, \quad (7)$$

where $y = \lambda'^2/8v = \lambda'^2/4v_r$ and $v_r = 2v$ is the relative velocity between the two dark matter particles. Taking the small v_r limit we have

$$R \approx \frac{\lambda'^2}{4v_r} \quad (8)$$

and we see that this effect will be largest for small v_r .

4 Calculation of the Relic Density

We are now in a position to calculate the relic density of our dark matter candidate. As mentioned in the previous section, in this paper we will restrict our analysis to dark matter particles with masses $m_{\tilde{s}} \geq 3 \text{ TeV}$. Not only is this range of masses physically interesting, it also simplifies the analysis considerably due to the fact that freeze-out occurs at a temperature above the electroweak phase transition, thus leading to a situation in which no scalars have vevs. Consequently, the number of possible vertices contributing to the annihilation cross sections is reduced and the calculation of the relic abundance greatly simplified.

There are three important types of diagram which determine the relic abundance of our dark matter particle. The first type (type I) involves the annihilation of two scalar s states. We can have two scalar s states annihilating into Higgs, Higgsinos, scalar n states or fermionic n states as depicted in Fig. 2. For computational ease we take all states to be massless apart from s and \tilde{s} which have masses $m_{\tilde{s}}$ and $m_{\tilde{s}} + m_{\text{susy}}^2/m_{\tilde{s}}$ respectively.

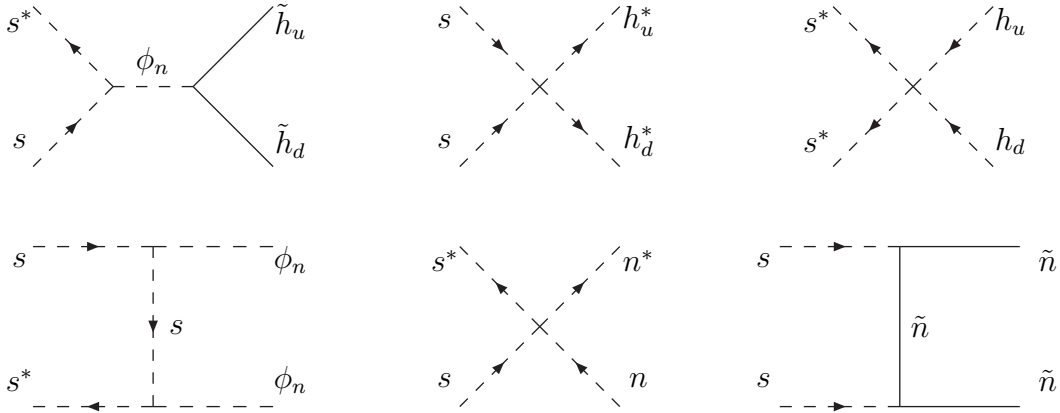


Figure 2: Type I annihilation diagrams for the scalar s states.

For all scalar annihilation diagrams we receive an enhancement from the Sommerfeld effect where the CP-even scalar, ϕ_n , acts as the “rungs on the ladder” between the annihilating scalar s states as depicted in Fig. 3 for the case of the annihilation of two s states. The “blob” vertex represents all possible ways of annihilating the s states including s-channel, t-channel and annihilation via the 4-point vertex.

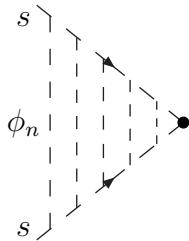


Figure 3: Sommerfeld diagram for scalar annihilations.

The resulting self annihilation cross sections for the CP-even and CP-odd components

of s are

$$\sigma(\phi_s\phi_s \rightarrow [\tilde{h}_u\tilde{h}_d]) = \sigma(a_s a_s \rightarrow [\tilde{h}_u\tilde{h}_d]) = \frac{(\lambda'\lambda)^2}{32\pi v_r m_{\tilde{s}}^2} \frac{y}{1 - e^{-y}}, \quad (9)$$

$$\sigma(\phi_s\phi_s \rightarrow [h_u h_d]) = \sigma(a_s a_s \rightarrow [h_u h_d]) = \frac{(\lambda'\lambda)^2}{32\pi v_r m_{\tilde{s}}^2} \frac{y}{1 - e^{-y}}, \quad (10)$$

$$\sigma(a_s\phi_s \rightarrow (h_u h_d)) = \frac{(\lambda'\lambda)^2}{16\pi v_r m_{\tilde{s}}^2} \frac{y}{1 - e^{-y}}, \quad (11)$$

$$\sigma(\phi_s\phi_s \rightarrow [nn]) = \sigma(a_s a_s \rightarrow [nn]) = \frac{\lambda'^4}{32\pi v_r m_{\tilde{s}}^2} \frac{y}{1 - e^{-y}}, \quad (12)$$

$$\sigma(\phi_s\phi_s \rightarrow \tilde{n}\tilde{n}) = \sigma(a_s a_s \rightarrow \tilde{n}\tilde{n}) = \frac{5\lambda'^4}{32\pi v_r m_{\tilde{s}}^2} \frac{y}{1 - e^{-y}}, \quad (13)$$

$$\sigma(\phi_s a_s \rightarrow \tilde{n}\tilde{n}) = \frac{\lambda'^4}{16\pi v_r m_{\tilde{s}}^2} \frac{y}{1 - e^{-y}}, \quad (14)$$

where the factor $y/(1 - e^{-y})$ accounts for the Sommerfeld enhancement and

$$\begin{aligned} [\tilde{h}_u\tilde{h}_d] &= \tilde{h}_u^0\tilde{h}_d^0, \tilde{h}_u^+\tilde{h}_d^-, (\tilde{h}_u^+\tilde{h}_d^-)^*, \\ [h_u h_d] &= \phi_u\phi_d, a_u a_d, h_u^+ h_d^-, (h_u^+ h_d^-)^*, \\ (h_u h_d) &= \phi_u a_d, a_u \phi_d, h_u^+ h_d^-, (h_u^+ h_d^-)^*, \\ [nn] &= \phi_n \phi_n, a_n a_n, \end{aligned}$$

represent all possible final states in each case.

The second type of diagram (type II) we need to include is the annihilation of a scalar s state with a fermionic \tilde{s} state. The relevant diagrams are shown in Fig. 4. Each process in Fig. 4 can also be enhanced by the Sommerfeld effect via the diagram shown in Fig. 5, where the ‘‘blob’’ vertex represents both s-channel and t-channel processes. The enhancement factor is exactly the same in this case as it was for the annihilation of scalar s states.

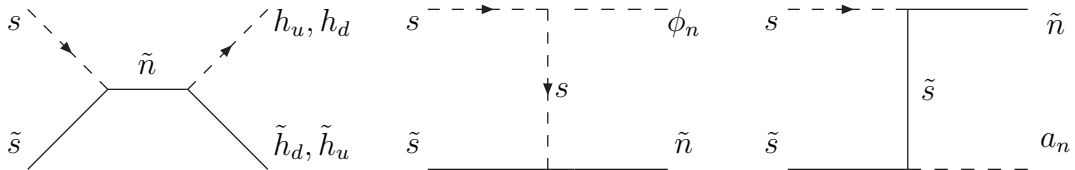


Figure 4: Type II: Annihilation of s with \tilde{s} .

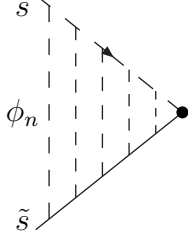


Figure 5: Sommerfeld diagrams for annihilation of s and \tilde{s} .

The cross sections for these processes are found to be

$$\sigma(\phi_s \tilde{s} \rightarrow (h_i \tilde{h}_j)) = \sigma(a_s \tilde{s} \rightarrow (h_i \tilde{h}_j)) = \frac{(\lambda' \lambda)^2}{32\pi v_r m_{\tilde{s}}^2} \frac{y}{1 - e^{-y}}, \quad (15)$$

$$\sigma(\phi_s \tilde{s} \rightarrow (n \tilde{n})) = \sigma(a_s \tilde{s} \rightarrow (n \tilde{n})) = \frac{(\lambda')^4}{32\pi v_r m_{\tilde{s}}^2} \frac{y}{1 - e^{-y}} \quad (16)$$

where

$$\begin{aligned} (h_i \tilde{h}_j) &= \phi_d \tilde{h}_u^0, a_d \tilde{h}_u^0, h_d^- \tilde{h}_u^+, (h_d^- \tilde{h}_u^+)^*, \phi_u \tilde{h}_d^0, a_u \tilde{h}_d^0, h_u^+ \tilde{h}_d^-, (h_u^+ \tilde{h}_d^-)^*, \\ (n \tilde{n}) &= a_n \tilde{n}, \phi_n \tilde{n}, \end{aligned}$$

represent all possible final states for each process.

The third type of process (type III) is the annihilation of the \tilde{s} states. In the electroweak symmetric limit, there are no vevs for the n or Higgs states, neither is there a tri-linear scalar A term, $A_\lambda n h_u h_d$ as we have approximated this term to be zero. This means that the only Higgs-like final states from \tilde{s} annihilation will be products of neutralinos and charginos. We can also have t-channel exchange of a \tilde{s} , which produces a CP-odd final state pair, $a_n \phi_n$. All possible diagrams with non-zero S -wave amplitudes are shown in Fig. 6.



Figure 6: Type III: Annihilation of two \tilde{s} states.

The $\tilde{s}\tilde{s}$ annihilation processes can be enhanced by the Sommerfeld factor if the initial \tilde{s} pair are in an S -wave state. The corresponding Sommerfeld diagram for $\tilde{s}\tilde{s}$ annihilation is shown in Fig. 7, where the “blob” vertex represents both s-channel and t-channel processes.

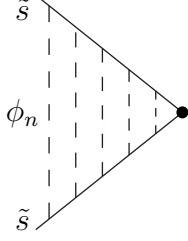


Figure 7: Sommerfeld diagrams for the annihilation of two \tilde{s} states.

The resulting cross sections for the \tilde{s} annihilations are found to be

$$\sigma(\tilde{s}\tilde{s} \rightarrow [\tilde{h}_u\tilde{h}_d]) = \frac{(\lambda'\lambda)^2}{64\pi v_r m_{\tilde{s}}^2} \frac{y}{1 - e^{-y}}, \quad (17)$$

$$\sigma(\tilde{s}\tilde{s} \rightarrow \tilde{n}\tilde{n}) = \frac{(\lambda')^4}{64\pi v_r m_{\tilde{s}}^2} \frac{y}{1 - e^{-y}} \quad (18)$$

where $[\tilde{h}_u\tilde{h}_d]$ was defined earlier in this section.

We now have all of the cross sections needed to determine the relic density. As we have two states freezing out almost simultaneously (our dark matter state \tilde{s} and its scalar partner s) we must be careful to include the effects of the heavier state in the calculation of the relic abundance of the dark matter species. We follow Refs. [24, 29] in calculating the final relic abundance of our dark matter candidate.

If we relabel our two states, \tilde{s} and s , as s_1 and s_2 respectively, the type of reaction that will determine the freeze-out of our two particles is

$$\sigma_{ij} = \sigma(s_i s_j \rightarrow X X'), \quad (19)$$

where X and X' will be some combination of Higgses, higgsinos, fermionic \tilde{n} states and scalar n states, which will decay to lighter MSSM degrees of freedom. Taking into account all possible diagrams, the three cross sections we are concerned with have the following forms

$$\sigma(s_1 s_1 \rightarrow X X') = \frac{[(\lambda'\lambda)^2 + (\lambda')^4]}{64\pi v_r m_{\tilde{s}}^2} \frac{y}{1 - e^{-y}}, \quad (20)$$

$$\sigma(s_1 s_2 \rightarrow X X') = \frac{[(\lambda'\lambda)^2 + (\lambda')^4]}{32\pi v_r m_{\tilde{s}}^2} \frac{y}{1 - e^{-y}}, \quad (21)$$

$$\sigma(s_2 s_2 \rightarrow X X') = \frac{[3(\lambda'\lambda)^2 + 7(\lambda')^4]}{64\pi v_r m_{\tilde{s}}^2} \frac{y}{1 - e^{-y}}, \quad (22)$$

where we have averaged over the components of the initial scalar states where appropriate.

We assume that any s_2 states remaining after freeze-out will eventually decay down to $s_1 X X'$. This means that the total number density of our dark matter particle will be equal to the sum of the s_1 and s_2 number densities at freeze-out.

In order to calculate the relic density we define the following useful quantities [24]

$$r_i \equiv \frac{g_i(1 + \Delta_i)^{3/2} \exp[-x\Delta_i]}{g_{\text{eff}}}, \quad (23)$$

where

$$\Delta_i = (m_i - m_1)/m_1, \quad (24)$$

and

$$g_{\text{eff}} = \sum_{i=1}^2 g_i(1 + \Delta_i)^{3/2} \exp[-x\Delta_i], \quad (25)$$

where g_i is the number of degrees of freedom of s_i , m_i is the mass of s_i and $x = m_{\tilde{s}}/T$. Of course in our case we only have two different species of particle and so only Δ_2 is non-zero. In fact as $s_1 = \tilde{s}$ and $s_2 = s$, we have $\Delta_2 = m_s - m_{\tilde{s}} \simeq m_{\text{susy}}^2/m_{\tilde{s}}$. Each of our s_i states have $g_i = 2$ degrees of freedom. Following Ref. [24], we find the freeze-out temperature, T_f , by iteratively solving the equation

$$x_f = \ln \left[\frac{0.038 g_{\text{eff}} M_{\text{pl}} m_{\tilde{s}} \langle \sigma_{\text{eff}} v_r \rangle}{g_{\star}^{1/2} x_f^{1/2}} \right], \quad (26)$$

where $x_f = m_{\tilde{s}}/T_f$ and

$$\sigma_{\text{eff}} = \sum_{i,j}^2 \sigma_{ij} r_i r_j = \sum_{i,j}^2 \sigma_{ij} \frac{g_i g_j}{g_{\text{eff}}^2} (1 + \Delta_i)^{3/2} (1 + \Delta_j)^{3/2} \exp(-x(\Delta_i + \Delta_j)). \quad (27)$$

The final relic density is given by [24]

$$\Omega h^2 = \frac{1.07 \times 10^9 x_f}{g_{\star}^{1/2} M_{\text{pl}} (\text{GeV}) J}, \quad \text{where } J = \int_{x_f}^{\infty} x^{-2} a_{\text{eff}} dx \quad (28)$$

and g_{\star} is the total number of relativistic degrees of freedom at T_f . In our calculation of the relic density we will take $g_{\star} = 248$, which includes all MSSM degrees of freedom plus the four associated with the extra superfield N . In order for this to be correct the masses of all these states must be below $T_f \sim m_{\tilde{s}}/25$, which will be true when we take $m_{\tilde{s}} \geq 3 \text{ TeV}$ and $m_{\text{susy}} = 100 \text{ GeV}$ as an example parameter set.

It is instructive to compare the two cases of when we correctly include the Sommerfeld factor in cross sections and when this contribution is absent. The comparison is most clear when we plot the relic density, $\Omega_{\tilde{s}} h^2$, against $m_{\tilde{s}}$ as shown in Fig. 8. In Fig. 8, the red dashed lines correspond to the case where the Sommerfeld factor (given by $R = y/(1 - e^{-y})$) is not included in the cross sections, while the blue solid lines correspond to the case where it is. The three lines for each case (with and without the Sommerfeld effect), starting from the furthest left, correspond to $\lambda = \lambda' = 2, 2.5, 3$ respectively. The two lines parallel with the $m_{\tilde{s}}$ axis correspond to the WMAP allowed range for the dark matter relic abundance, inferred from the combination of $\Omega_M h^2 = 0.1277_{-0.0079}^{+0.0080}$ and $\Omega_b h^2 = 0.02229 \pm 0.00073$ [30].

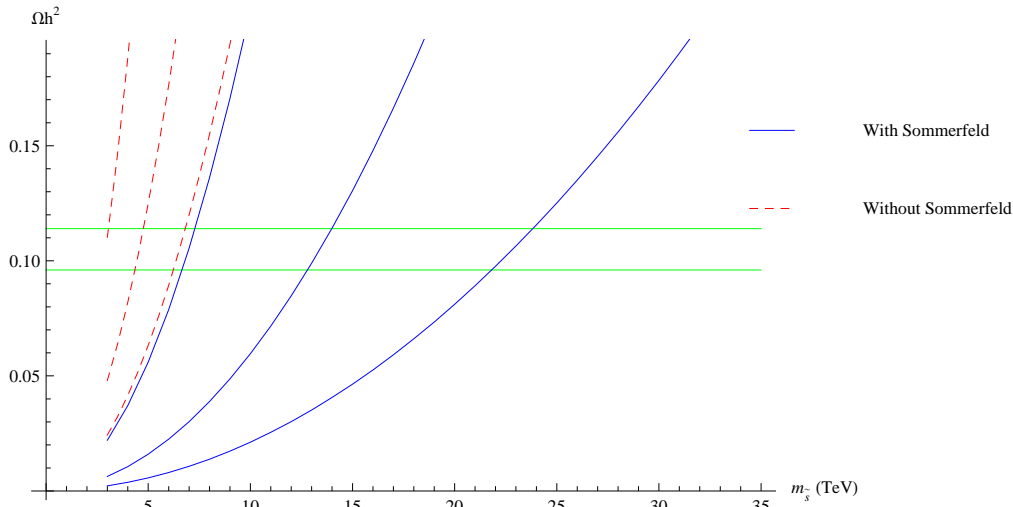


Figure 8: Ωh^2 as function of $m_{\tilde{s}}$ at fixed λ and λ' . The red dashed lines correspond to the case where the Sommerfeld correction is not included where as the blue solid lines correspond to the case when it is included. The furthest most left line for each colour corresponds to when $\lambda = \lambda' = 2$, the middle lines are when $\lambda = \lambda' = 2.5$ and the lines furthest right are when $\lambda = \lambda' = 3$. All plots are produced using $m_{\text{susy}} = 100$ GeV.

For each line (of fixed coupling), the relic density increases as we increase the mass, $m_{\tilde{s}}$, as we would expect. Comparing sets of contours with the same couplings ($\lambda = \lambda'$), we see the dramatic effect of the Sommerfeld enhancement. When the Sommerfeld enhancement is included, the annihilation cross sections are increased, thus depleting the number density of the dark matter particles which survive after freeze-out. The bottom line is that the Sommerfeld enhancement allows for very heavy dark matter particles to provide the required dark matter relic abundance. From Fig. 8 we can see that the maximum mass consistent with the WMAP allowed range when we have $\lambda = \lambda' = 3$ is close to 25 TeV.

The results of a full numerical scan (including the Sommerfeld enhancement) over the three parameters λ, λ' and $m_{\tilde{s}}$ is shown in Fig. 9. Here, we plot contours corresponding to the allowed range of $\Omega_{\tilde{s}} h^2$ in the $\lambda - \lambda'$ plane. Each pair of contours correspond to a different value of the mass, $m_{\tilde{s}}$, between 3 and 23 TeV. The left (right) contour of each pair corresponds to the higher (lower) end of the allowed range in $\Omega_{\tilde{s}} h^2$.

Although we show contours only for discrete choices of $m_{\tilde{s}}$, the remaining regions of the $\lambda - \lambda'$ plane are filled for intermediate values of the dark matter mass.⁷ The effect of the Sommerfeld enhancement is to pull the pairs of contours downward towards the bottom left corner of the $\lambda - \lambda'$ plane. This allows us to have the correct relic density for a given dark matter mass for smaller values of the couplings.

On examination of the parameter region shown in Fig. 9, it is interesting and perhaps

⁷There will be an upper limit on how large the couplings can be, which is determined by insisting we have perturbativity up to our cut off scale. As shown in Section 6, large couplings of the size considered here are shown to be natural in a consistent UV completion.

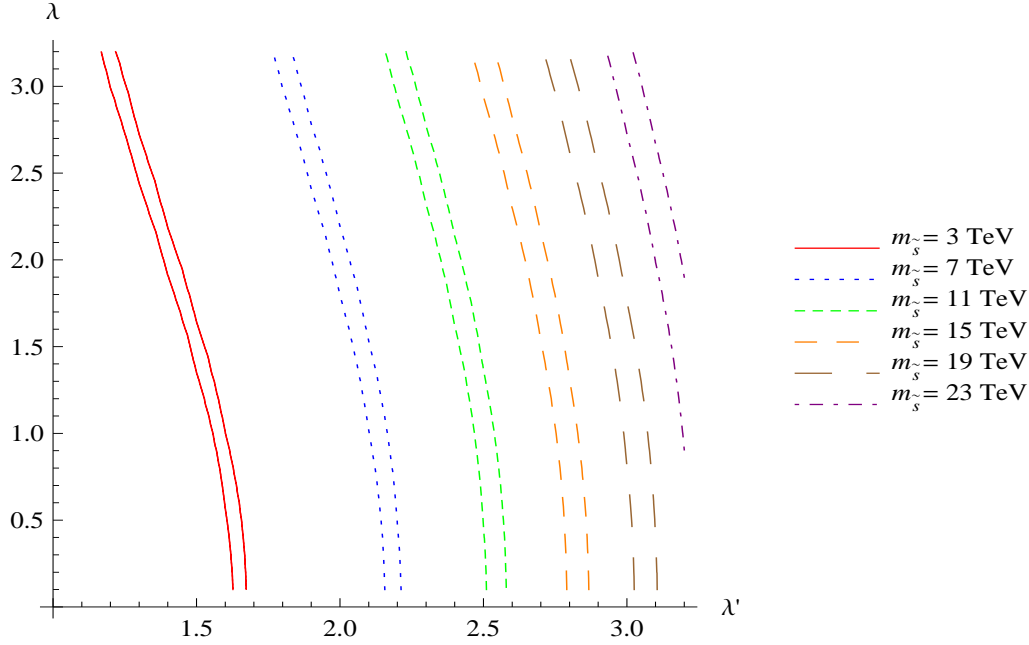


Figure 9: Plots of pairs of contours for the allowed range of Ωh^2 in the $\lambda - \lambda'$ parameter plane for different values of the mass, $m_{\tilde{g}}$. We have contours corresponding to masses 3, 7, 11, 15, 19, 23 TeV. The contours are produced using $m_{\text{susy}} = 100 \text{ GeV}$.

important to note that we are able to generate the correct dark matter relic density (for a given mass) for relatively small λ couplings, provided we have a large enough λ' coupling. The main reason for this is that only the λ' coupling appears in the Sommerfeld enhancement and as we can see from Fig. 8, it is the Sommerfeld enhancement that allows us to have large masses for the dark matter particles. With this in mind, it is also interesting to note that as we have annihilation diagrams which depend on λ' only, we can take λ to be small (around 0.1 for example) and still have viable dark matter with masses up to around 23 TeV.

5 Direct and Indirect Detection

Although we intend to discuss the prospects for the direct and indirect detection of heavy Higgs Portal dark matter in some detail in a companion paper to follow [17] we will here briefly touch upon this subject. We find that the direct detection phenomenology is fairly conventional and, although present experiments do not yet lead to restrictive limits, a sizeable fraction of the expected parameter space will be covered by proposed next generation detectors. In contrast, the indirect signals are greatly modified by the potentially very large Sommerfeld enhancements.

5.1 Direct Detection

Experimental programs designed to observe the elastic scattering of WIMPs with nuclei are collectively known as direct detection. The dark matter particles in our model, \tilde{s} , interact with quarks in nuclei through the effective scalar interaction given by

$$\mathcal{L} = \sum_{U=u,c,t} C_U \tilde{s}\tilde{s}\bar{U}U + \sum_{D=d,s,b} C_D \tilde{s}\tilde{s}\bar{D}D, \quad (29)$$

where

$$C_U = \sum_i \frac{\lambda_U V_{1i} V_{2i} \lambda'}{2m_{h_i}^2} \text{ and } C_D = \sum_i \frac{\lambda_D V_{1i} V_{3i} \lambda'}{2m_{h_i}^2}, \quad (30)$$

and the mixing matrix V_{ij} specifies the admixture of n , h_u^0 , and h_d^0 states in the neutral scalar mass eigenstates, h_i , with lightest neutral Higgs state being denoted h_1 . Unlike in the case of many other dark matter candidates, there is no contribution from Z exchange in this model. Note that the kinematics of the interaction (even if we consider scattering of individual nucleons or even quarks with the dark matter) are such that we are outside of the range for which the Sommerfeld enhancement is important.

Following Refs. [31, 23], we estimate that this interaction leads to an elastic scattering cross section per nucleon of

$$\sigma_{\tilde{s}N} \sim 2 \times 10^{-7} \text{ pb} \left(\frac{V_{ij}}{0.5} \right)^4 \left(\frac{\lambda'}{3} \right)^2 \left(\frac{120 \text{ GeV}}{m_{h_1}} \right)^4. \quad (31)$$

For the range of masses we are interested in here, this cross section is below the current constraints from experiments such as XENON [32] and CDMS [33], but is likely to be reached in the next few years. For less optimal values of λ' , m_{h_1} or V_{ij} , however, the prospects for direct detection could be considerably more difficult.

5.2 Indirect Detection

In addition to direct searches for dark matter, astronomers are also searching for the products of dark matter annihilations, including gamma-rays, neutrinos, positrons and antiprotons [34]. These efforts are known as indirect detection.

The dark matter annihilation rate, and thus indirect detection rates, can be enormously enhanced due to the Sommerfeld effect. Depending on the astrophysical environment being considered, annihilation rates can be enhanced by factors of 10^3 to 10^5 or even greater due to the slow relative velocities of dark matter particles. In fact, the velocity dependence of the enhancement factor can potentially favour such astrophysical objects as dwarf satellite galaxies of the Milky Way (due to the extremely low velocity dispersion) as sites for indirect detection, rather than the central regions of the Milky Way itself. A full calculation of the expected flux depends upon a detailed knowledge both of the resonance structure of the Sommerfeld enhancement in the non-coulombic and low v_r regime and of the sizes of vacuum expectation values and interaction terms

in the scalar (S, N) -Higgs sector. A preliminary estimate shows that current indirect detection experiments do not impose a useful limit on heavy Higgs portal dark matter, but that there is a potential for significant signals in future observations [17].

6 UV Completion as a Fat Higgs Model

It should be noted that the sizes of the couplings we have taken in the analysis of section 4 are the values for typical momentum transfers at freeze-out ($\sim m_{\tilde{s}}\beta_{fo}$, with $\beta_{fo} \sim 0.2$). The cut-off of our effective theory will be related to the energy scale at which our couplings become non-perturbative, which for definiteness we take to be where the two loop terms in the renormalisation group equations for λ and λ' become of order the one loop terms. For example, if we take $m_{\tilde{s}} = 3 \text{ TeV}$, $\lambda = 0.8$ and $\lambda' = 1.6$ the cut-off is $\sim 4000 \text{ TeV}$. A more extreme example is where we take $m_{\tilde{s}} = 23 \text{ TeV}$, $\lambda = 1.0$ and $\lambda' = 3.2$ with cut-off $\sim 70 \text{ TeV}$. The consequence of having a cut-off below the GUT scale is that we are motivated to think about how this model can be UV completed. We emphasise that for the analysis of the dark matter properties and thermal freeze out the effective low energy lagrangian, Eq.(1), is appropriate as there is a large separation between $m_{\tilde{s}}\beta_{fo}$ and the cut-off even for the most extreme case we consider, $m_{\tilde{s}} = 23 \text{ TeV}$.

One possible way to UV complete our model and justify the choice of large couplings λ, λ' is to have some strongly interacting physics which dynamically generates the superpotential S mass. It is noteworthy that the ‘‘Fat Higgs model’’ of Ref. [18] provides exactly such a UV completion. With this in mind, we will now describe how our effective theory can arise in a certain limit of the Fat Higgs models.

The Fat Higgs model is an $N = 1$ supersymmetric $SU(2)$ gauge theory with six doublets with the quantum numbers shown in Table 1.

The tree-level superpotential is given as⁸ $W_{\text{FHtot}} = W_1 + W_2 + W_3$ where

$$W_1 = y_1 S_1 T_1 T_2 + y_2 S_2 T_3 T_4 + y_3 S_1 T_3 T_4 + y_4 S_2 T_1 T_2 \quad (32)$$

$$W_2 = -m T_5 T_6 \quad (33)$$

$$W_3 = y_5 \begin{pmatrix} T_1 & T_2 \end{pmatrix} P \begin{pmatrix} T_5 \\ T_6 \end{pmatrix} + y_6 \begin{pmatrix} T_3 & T_4 \end{pmatrix} Q \begin{pmatrix} T_5 \\ T_6 \end{pmatrix}. \quad (34)$$

The P and Q mixing terms are there to marry off unwanted ‘‘spectator’’ states such that the low energy effective theory is as minimal as possible. It is also possible to apply a Z_3 which protects us from tadpole terms involving either of the singlet fields, S_1 and S_2 [18]. This Z_3 will commute with the existing symmetries.

The gauge symmetry $SU(2)_H$ becomes strongly coupled at some scale, Λ_H . Below Λ_H , the appropriate degrees of freedom are mesons which are composite objects consisting of two ‘‘T’’ doublets in the form $M_{ij} = T_i T_j$, with $(i, j=1\dots 6)$. There is a dynamically generated superpotential of the form $\text{Pf}M/\Lambda_H^3$ as well as the tree level superpotential

⁸The terms with coefficients y_3 and y_4 were not included in Ref. [18]. These terms are not forbidden by any symmetries so we include them for completeness.

Superfield	$SU(2)_L$	$SU(2)_H$	$SU(2)_R$	$SU(2)_g$	$U(1)_R$	Z_2
T_1	2	2	1	1	0	+
T_2	2	2	1	1	0	-
T_3	1	2	2	1	1	-
T_4	1	2	2	1	1	+
T_5	1	2	1	2	1	+
T_6	1	2	1	2	1	+
P_{11}	2	1	1	2	1	+
P_{12}	2	1	1	2	1	+
P_{21}	2	1	1	2	1	-
P_{22}	2	1	1	2	1	-
Q_{11}	1	1	2	2	1	-
Q_{12}	1	1	2	2	1	-
Q_{21}	1	1	2	2	1	+
Q_{22}	1	1	2	2	1	+
S_1	1	1	1	1	2	-
S_2	1	1	1	1	2	-

Table 1: The field content under an $SU(2)_L \times SU(2)_H$ gauge and $SU(2)_R \times SU(2)_g \times U(1)_R$ global symmetries. There is also an accidental Z_2 symmetry with fields transforming as shown. The $U(1)_Y$ subgroup of $SU(2)_R$ is gauged.

which follows from Eq.(34). As P, Q, S_1 and S_2 are not charged under $SU(2)_H$, they remain fundamental below Λ_H . The canonically normalised effective superpotential reads

$$\begin{aligned}
W_{dyn} &= \lambda (\text{Pf}M - v_0^2 M_{56}) + m_1 S_1 M_{12} + m_2 S_2 M_{34} + m_3 S_1 M_{34} + m_4 S_2 M_{12} \\
&+ m_5 (M_{15} P_{11} + M_{16} P_{12} + M_{25} P_{21} + M_{26} P_{22}) \\
&+ m_6 (M_{35} Q_{11} + M_{36} Q_{12} + M_{45} Q_{21} + M_{36} Q_{22}), \tag{35}
\end{aligned}$$

where, using Naive Dimensional Analysis (NDA) [35], we have

$$v_0^2 \sim \frac{m \Lambda_H}{(4\pi)^2}, \tag{36}$$

$$m_i \sim y_i \frac{\Lambda_H}{4\pi}, \tag{37}$$

$$\lambda(\Lambda_H) \sim 4\pi. \tag{38}$$

We now make the assumption that $(m_5, m_6) \gg (m_1, m_2, m_3, m_4)$, by a factor of 10 or so, and integrate out everything with a mass proportional to m_5 or m_6 . This leaves us with a superpotential of the form

$$\begin{aligned}
W'_{dyn} &= \lambda M_{56} (M_{14} M_{23} - M_{24} M_{13} - v_0^2 + M_{12} M_{34}) \\
&+ m_1 S_1 M_{12} + m_2 S_2 M_{34} + m_3 S_1 M_{34} + m_4 S_2 M_{12}. \tag{39}
\end{aligned}$$

Assuming that $m_1 \sim m_2 \sim m_3 \sim m_4 \sim m'$, the fermionic components of the superfields, S_1, S_2, M_{12} and M_{34} , mix and, provided $m_1 m_2 \neq m_3 m_4$, the lightest eigenvalue of this mass matrix will generically have a mass of order m' .

If we now do this diagonalization and integrate out all but the lightest eigenvalue, call it S , of the S_1, S_2, M_{12}, M_{34} mass matrix, we are left with the superpotential

$$W = \lambda N (H_u H_d - v_0^2) + \frac{\lambda'}{2} N S^2 + \frac{m_{\tilde{s}}}{2} S^2, \quad (40)$$

where we have changed notation according to the identifications

$$\begin{pmatrix} H_u^+ \\ H_u^0 \end{pmatrix} = \begin{pmatrix} M_{13} \\ M_{23} \end{pmatrix}, \quad \begin{pmatrix} H_d^0 \\ H_d^- \end{pmatrix} = \begin{pmatrix} M_{14} \\ M_{24} \end{pmatrix}, \quad N = M_{56}. \quad (41)$$

The parameter $\lambda' = \lambda U_{ij} U_{kl}$, where $U_{ij} U_{kl}$ are components of the unitary matrix that diagonalizes the S_1, S_2, M_{12}, M_{34} fermion mass matrix. The indices on the U s are there for show, the basis is irrelevant as we do not really care about the specific mixing between states.

The final assumption we make is that $m_{\tilde{s}}$ is parametrically larger than the electroweak scale and soft supersymmetry breaking masses. The superpotential in Eq.(41) is of the form we need with an additional linear term for the superfield N . This term is harmless with respect to the dark matter dynamics but we include it for completeness.

Ignoring the S field for now, the remaining superpotential is that of the Fat Higgs model and the analysis of the electroweak vacuum structure proceeds as outlined in Ref. [18]. It is worth comparing the superpotential in Eq.(41) with that of the MNSSM [27, 28]. In particular, the N linear term in Eq.(41) is analogous to the tadpole terms appearing in the superpotential of Eq.(3.1) of Ref. [27]. In fact, the superpotential in Eq.(41) (apart from the S terms) is that of the MNSSM. Consequently we can use the rather more detailed analysis of Refs. [27, 28] for the Higgs sector.

The S terms in Eq.(41) do not spoil the electroweak structure of the MNSSM. We can see this by integrating out S using the equations of motion

$$\frac{\partial W}{\partial S} = \lambda' N S + m_{\tilde{s}} S = 0, \quad \Rightarrow \quad S = 0. \quad (42)$$

Substituting the solution back into Eq.(41) we have the effective superpotential

$$W_{\text{eff}} = \lambda N (H_u H_d - v_0^2), \quad (43)$$

which is exactly the same as the superpotential for the MNSSM and the Fat Higgs model.

7 Conclusions

In this article, we have discussed models in which a very heavy (3-30 TeV) dark matter candidate is present. In particular, we have focused on models motivated by Higgs Portal and Hidden Valley models, in which the dark matter (and the rest of the partially hidden sector) interacts with the Standard Model and its superpartners only through Higgs interactions.

Dark matter annihilations in this scenario are considerably enhanced by non-perturbative contributions known as the Sommerfeld effect. Through this enhancement, dark matter particles with masses well above the electroweak scale can be produced thermally in the early universe with an abundance consistent with the measured density of dark matter. The dark matter particle in this scenario, although well beyond the reach of the Large Hadron Collider, is still potentially detectable by direct and indirect dark matter experiments. Although we leave the details of this to future work [17], we point out that Sommerfeld corrections can dramatically enhance the dark matter annihilation rate in low velocity dispersion environments, such as dwarf spheroidal galaxies, thus considerably improving the prospects for indirect dark matter searches.

The particular model we study, which adds two extra SM singlet states to the MSSM spectrum, is independently motivated by the desire to raise the upper bound on the lightest higgs mass, thus lessening the LEP fine-tuning constraints. We also showed that our model may be given a UV completion in the form of the previously considered “Fat Higgs” models, where the singlet states are composites arising from strong hidden-sector dynamics.

Thus, Higgs Portal Dark Matter provides an example of an attractive and motivated alternative to conventional MSSM neutralino dark matter which is less fine-tuned and may be tested by current and future indirect detection experiments.

Acknowledgements JMR and SMW are partially supported by the EC Network 6th Framework Programme Research and Training Network “Quest for Unification” (MRTN-CT-2004-503369) and by the EU FP6 Marie Curie Research and Training Network “UniverseNet” (MPRN-CT-2006-035863). DC is supported by the Science and Technology Facilities Council. DH is supported by the United States Department of Energy and NASA grant NAG5-10842. Fermilab is operated by the Fermi Research Alliance, LLC under Contract No. DE-AC02-07CH11359 with the United States Department of Energy. We would like to thank Markus Ahlers, Joe Silk, and Tim Tait for useful discussions.

References

- [1] M. J. Strassler and K. M. Zurek, Phys. Lett. B **651** (2007) 374 [arXiv:hep-ph/0604261]; M. J. Strassler and K. M. Zurek, arXiv:hep-ph/0605193; J. Kumar and J. D. Wells, Phys. Rev. D **74** (2006) 115017 [arXiv:hep-ph/0606183]; M. J. Strassler, arXiv:hep-ph/0607160; T. Han, *et al.*, arXiv:0712.2041 [hep-ph]; M. J. Strassler, arXiv:0801.0629 [hep-ph].
- [2] F. Wilczek, Czech. J. Phys. **54** (2004) A415 [arXiv:hep-ph/0401126].
- [3] R. Schabinger and J. D. Wells, Phys. Rev. D **72** (2005) 093007 [arXiv:hep-ph/0509209].
- [4] B. Patt and F. Wilczek, arXiv:hep-ph/0605188.

- [5] X. Calmet and J. F. Oliver, *Europhys. Lett.* **77** (2007) 51002 [arXiv:hep-ph/0606209]; G. Burdman, *et al.*, *JHEP* **0702** (2007) 009 [arXiv:hep-ph/0609152]; D. G. Cerdeno, A. Dedes and T. E. J. Underwood, *JHEP* **0609** (2006) 067 [arXiv:hep-ph/0607157]; P. H. Gu and H. J. He, *JCAP* **0612** (2006) 010 [arXiv:hep-ph/0610275]; M. Bowen, Y. Cui and J. D. Wells, *JHEP* **0703** (2007) 036 [arXiv:hep-ph/0701035]; J. R. Espinosa and M. Quiros, *Phys. Rev. D* **76** (2007) 076004 [arXiv:hep-ph/0701145]; D. E. Kaplan and K. Rehermann, *JHEP* **0710** (2007) 056 [arXiv:0705.3426 [hep-ph]]; V. Barger, *et al.*, arXiv:0706.4311 [hep-ph]; O. Bertolami and R. Rosenfeld, arXiv:0708.1784 [hep-ph]. R. A. Porto and A. Zee, arXiv:0712.0448 [hep-ph]; G. Bhattacharyya, G. C. Branco and S. Nandi, arXiv:0712.2693 [hep-ph].
- [6] W. F. Chang, J. N. Ng and J. M. S. Wu, *Phys. Rev. D* **74** (2006) 095005 [arXiv:hep-ph/0608068]; *Phys. Rev. D* **75** (2007) 115016 [arXiv:hep-ph/0701254]; and arXiv:0706.2345 [hep-ph]; S. Gopalakrishna, S. Jung and J. D. Wells, arXiv:0801.3456 [hep-ph].
- [7] B. Holdom, *Phys. Lett. B* **166** (1986) 196; F. del Aguila, G. D. Coughlan and M. Quiros, *Nucl. Phys. B* **307** (1988) 633 [Erratum-ibid. **B 312** (1989) 751]; K. S. Babu, C. F. Kolda and J. March-Russell, *Phys. Rev. D* **57** (1998) 6788 [arXiv:hep-ph/9710441]; K. R. Dienes, C. F. Kolda and J. March-Russell, *Nucl. Phys. B* **492** (1997) 104 [arXiv:hep-ph/9610479]; K. S. Babu, C. F. Kolda and J. March-Russell, *Phys. Rev. D* **54** (1996) 4635 [arXiv:hep-ph/9603212];
- [8] S. Dimopoulos, G. F. Giudice and A. Pomarol, *Phys. Lett. B* **389** (1996) 37 [arXiv:hep-ph/9607225]; T. Han and R. Hempfling, *Phys. Lett. B* **415** (1997) 161 [arXiv:hep-ph/9708264]; T. Han, D. Marfatia and R. J. Zhang, *Phys. Rev. D* **61** (2000) 013007 [arXiv:hep-ph/9906508]; D. Hooper and J. March-Russell, *Phys. Lett. B* **608** (2005) 17 [arXiv:hep-ph/0412048];
- [9] K. Cheung and T. C. Yuan, *JHEP* **0703** (2007) 120 [arXiv:hep-ph/0701107]; T. Hambye and M. H. G. Tytgat, arXiv:0707.0633 [hep-ph]; O. Bertolami and R. Rosenfeld, arXiv:0708.1784 [hep-ph]; T. Hur, D. W. Jung, P. Ko and J. Y. Lee, arXiv:0709.1218 [hep-ph]; K. Petraki and A. Kusenko, arXiv:0711.4646 [hep-ph]; M. Pospelov, A. Ritz and M. B. Voloshin, arXiv:0711.4866 [hep-ph]; W. Krolikowski, arXiv:0712.0505 [hep-ph].
- [10] J. McDonald, *Phys. Rev. D* **50** (1994) 3637 [arXiv:hep-ph/0702143]; V. Silveira and A. Zee, *Phys. Lett. B* **161** (1985) 136; D. E. Holz and A. Zee, *Phys. Lett. B* **517** (2001) 239 [arXiv:hep-ph/0105284]; J. McDonald, *Phys. Rev. Lett.* **88** (2002) 091304 [arXiv:hep-ph/0106249]; C. P. Burgess, M. Pospelov and T. ter Veldhuis, *Nucl. Phys. B* **619** (2001) 709 [arXiv:hep-ph/0011335]; M. Cirelli, N. Fornengo and A. Strumia, *Nucl. Phys. B* **753** (2006) 178 [arXiv:hep-ph/0512090]; Y. G. Kim and K. Y. Lee, *Phys. Rev. D* **75** (2007) 115012 [arXiv:hep-ph/0611069]; H. Sung Cheon, S. K. Kang and C. S. Kim, arXiv:0710.2416 [hep-ph].
- [11] K. Griest and M. Kamionkowski, *Phys. Rev. Lett.* **64**, 615 (1990);

- [12] A. Sommerfeld, Ann. Phys. 11 257 (1931)
- [13] H. Baer, K. m. Cheung and J. F. Gunion, Phys. Rev. D **59** (1999) 075002 [arXiv:hep-ph/9806361].
- [14] J. Hisano, S. Matsumoto and M. M. Nojiri, Phys. Rev. D **67**, 075014 (2003) [arXiv:hep-ph/0212022]; J. Hisano, S. Matsumoto and M. M. Nojiri, Phys. Rev. Lett. **92**, 031303 (2004) [arXiv:hep-ph/0307216]; J. Hisano, *et al.*, Phys. Rev. D **71**, 015007 (2005) [arXiv:hep-ph/0407168]; J. Hisano, *et al.*, Phys. Rev. D **71**, 063528 (2005) [arXiv:hep-ph/0412403]; J. Hisano, *et al.* Phys. Rev. D **73**, 055004 (2006) [arXiv:hep-ph/0511118]; J. Hisano, *et al.*, Phys. Lett. B **646** (2007) 34 [arXiv:hep-ph/0610249].
- [15] S. Profumo, “TeV gamma-rays and the largest masses and annihilation cross sections of neutralino DM,” Phys. Rev. D **72** (2005) 103521 [arXiv:astro-ph/0508628].
- [16] M. Cirelli, A. Strumia and M. Tamburini, Nucl. Phys. B **787** (2007) 152 [arXiv:0706.4071 [hep-ph]].
- [17] D. Cumberbatch, D. Hooper, J. March-Russell and S. M. West, In Preparation, OUTP-08-01P.
- [18] R. Harnik, *et al.*, Phys. Rev. D **70** (2004) 015002 [arXiv:hep-ph/0311349].
- [19] S. Chang, C. Kilic and R. Mahbubani, Phys. Rev. D **71** (2005) 015003 [arXiv:hep-ph/0405267]; A. Delgado and T. M. P. Tait, JHEP **0507** (2005) 023 [arXiv:hep-ph/0504224]; C. Liu, Mod. Phys. Lett. A **15** (2000) 525 [arXiv:hep-ph/9903395].
- [20] See, for example, M. Cvetič and P. Langacker, Phys. Rev. D **54** (1996) 3570 [arXiv:hep-ph/9511378]; and J. L. Hewett and T. G. Rizzo, Phys. Rept. **183** (1989) 193.
- [21] L. Randall and R. Sundrum, Phys. Rev. Lett. **83** (1999) 3370 [arXiv:hep-ph/9905221]; and Phys. Rev. Lett. **83** (1999) 4690 [arXiv:hep-th/9906064]; H. L. Verlinde, Nucl. Phys. B **580** (2000) 264 [arXiv:hep-th/9906182]; C. S. Chan, P. L. Paul and H. L. Verlinde, Nucl. Phys. B **581** (2000) 156 [arXiv:hep-th/0003236]; S. Dimopoulos, *et al.*, Phys. Rev. D **64** (2001) 121702 [arXiv:hep-th/0104239]; S. B. Giddings, S. Kachru and J. Polchinski, Phys. Rev. D **66** (2002) 106006 [arXiv:hep-th/0105097]; S. Dimopoulos, *et al.*, Int. J. Mod. Phys. A **19** (2004) 2657 [arXiv:hep-th/0106128]; M. Grana, Phys. Rept. **423** (2006) 91 [arXiv:hep-th/0509003]; G. Cacciapaglia, *et al.*, Phys. Rev. D **74** (2006) 045019 [arXiv:hep-ph/0604218].
- [22] A. Hebecker and J. March-Russell, Nucl. Phys. B **781**, 99 (2007) [arXiv:hep-th/0607120].
- [23] G. Jungman, M. Kamionkowski and K. Griest, Phys. Rept. **267** (1996) 195 [arXiv:hep-ph/9506380].

- [24] K. Griest and D. Seckel, Phys. Rev. D **43** (1991) 3191.
- [25] S. Dimopoulos, *et al.*, Astrophys. J. **330** (1988) 545; and Nucl. Phys. B **311** (1989) 699. M. Kawasaki, K. Kohri and T. Moroi, Phys. Lett. B **625** (2005) 7 [arXiv:astro-ph/0402490]; and Phys. Rev. D **71** (2005) 083502 [arXiv:astro-ph/0408426]; K. Jedamzik, Phys. Rev. D **70** (2004) 063524 [arXiv:astro-ph/0402344]; and Phys. Rev. D **74** (2006) 103509 [arXiv:hep-ph/0604251]; D. Cumberbatch, *et al.*, Phys. Rev. D **76**, 123005 (2007) [arXiv:0708.0095 [astro-ph]].
- [26] B. Gripaios and S. M. West, Phys. Rev. D **74**, 075002 (2006) [arXiv:hep-ph/0603229]; J. A. Casas, J. R. Espinosa and I. Hidalgo, Nucl. Phys. B **777** (2007) 226 [arXiv:hep-ph/0607279]; S. Chang, P. J. Fox and N. Weiner, Phys. Rev. Lett. **98** (2007) 111802 [arXiv:hep-ph/0608310]; R. Dermisek and J. F. Gunion, Phys. Rev. D **75** (2007) 075019 [arXiv:hep-ph/0611142].
- [27] C. Panagiotakopoulos and A. Pilaftsis, Phys. Rev. D **63** (2001) 055003 [arXiv:hep-ph/0008268].
- [28] A. Dedes, *et al.*, Phys. Rev. D **63** (2001) 055009 [arXiv:hep-ph/0009125].
- [29] P. Gondolo and G. Gelmini, Nucl. Phys. B **360** (1991) 145.
- [30] D. N. Spergel, *et al.*, [WMAP Collaboration], Astrophys. J. Suppl. **170** (2007) 377 [arXiv:astro-ph/0603449].
- [31] K. Griest, Phys. Rev. D **38**, 2357 (1988) [Erratum-ibid. D **39**, 3802 (1989)]; R. Barbieri, M. Frigeni and G. F. Giudice, Nucl. Phys. B **313**, 725 (1989).
- [32] J. Angle *et al.* [XENON Collaboration], arXiv:0706.0039 [astro-ph].
- [33] D. S. Akerib, *et al.*, [CDMS Collaboration], arXiv:astro-ph/0509259.
- [34] G. Bertone, D. Hooper and J. Silk, Phys. Rept. **405**, 279 (2005) [arXiv:hep-ph/0404175].
- [35] M. A. Luty, Phys. Rev. D **57** (1998) 1531 [arXiv:hep-ph/9706235].